

Reactions and Reaction Intermediates on Iron Surfaces

I. Methanol, Ethanol, and Isopropanol on Fe(100)

J. B. BENZIGER¹ AND R. J. MADIX*Department of Chemical Engineering, Stanford University, Stanford, California 94305*

Received September 13, 1979; revised March 4, 1980

The reactions of methanol, ethanol, and isopropanol on an Fe(100) surface were studied using temperature-programmed reaction spectroscopy (TPRS) and X-ray photoelectron spectroscopy (XPS). Methanol and ethanol readily formed alkoxy intermediates at or below room temperature by loss of the hydroxyl hydrogens. These alkoxy species reacted above 400 K in three ways: (i) complete decomposition to CO and hydrogen, (ii) rehydrogenation to the alcohol, and (iii) scission of the C-C or C-O bonds with hydrogenation of the hydrocarbon fragment. All these reactions appeared to occur simultaneously and proceeded with first-order kinetics. The first-order rate constants for reactions of the methoxy and ethoxy species were determined to be

$$k_{\text{CH}_3\text{O}} = (4 \times 10^{12}) \exp(-105 \text{ kJ/mole}/RT) \text{ s}^{-1}$$

$$k_{\text{C}_2\text{H}_5\text{O}} = (8 \times 10^{13}) \exp(-111 \text{ kJ/mole}/RT) \text{ s}^{-1},$$

respectively. Isopropanol reacted differently from either methanol or ethanol; it did not readily form a stable alkoxy intermediate. The difference in the reactions of primary and secondary alcohols was suggested to arise from steric interference of the methyl groups with the surface. These results were consistent with the results of Kummer and Emmett, which showed alcohol-related intermediates were important in Fischer-Tropsch synthesis. These observations also showed that alkoxy intermediates must be considered as possible routes in the Fischer-Tropsch synthesis.

INTRODUCTION

Reaction mechanisms and kinetics in organic chemistry of the gas or liquid phases can often be understood in terms of certain well-defined reaction intermediates. The stability and reaction mechanisms of these intermediates can be correlated with their structures (1). However, the understanding of reactions occurring on solid surfaces is in a much more primitive state of development. The reason for our lack of understanding of surface reactions is that relatively little is known about the identity of surface species, and even less about their reactions.

With modern surface science techniques

¹ Current address: Department of Chemical Engineering, Princeton University, Princeton, New Jersey 08540.

it has become possible to identify surface intermediates and the reactions of these intermediates (2). We have examined a number of reactions on Fe(100) utilizing both temperature-programmed reaction spectroscopy (TPRS) and X-ray photoelectron spectroscopy (XPS) to identify surface intermediates and follow their reactions. In this paper the reactions of alcohols on an Fe(100) surface are presented. Certain classes of stable surface intermediates were observed which have analogs in other branches of chemistry. Furthermore, the stability of these intermediates appears to be related to their structure. In subsequent papers reactions of hydrocarbons, carboxylic acids, aldehydes, and ketones will be discussed, and it will be shown that the overall thermodynamics of the surface reactions can be employed to explain trends

in the reactions on different metals. The last paper in the series will relate the results for reactions on iron surfaces to the Fischer-Tropsch synthesis.

The reactions of alcohols on iron have been a neglected area of study even though alcohols have been observed to be a major product from CO hydrogenation reactions over iron catalysts (3). Kummer and Emmett (4) found that when primary alcohols were added to a CO/H₂ feed stream and passed over iron catalysts, they led to growth of long-chain hydrocarbons. The observations of Kummer and Emmett led Anderson and co-workers (5) to propose that alcohols adsorbed on the surface as an

enol type intermediate ($* = \text{C} \begin{array}{l} \text{H} \\ \diagup \\ \text{OH} \end{array}$) which

polymerized by water elimination to form larger chains. The role of this type of intermediate was questioned by the work of Blyholder and Neff, from which the infrared absorption spectra of alcohols adsorbed on iron powders suggested that alkoxide intermediates ($*-\text{OR}$) (6) were important. Despite the obvious importance of alcohol-related intermediates in the Fischer-Tropsch synthesis there seem to be no studies of the reactions of alcohols over iron catalysts. It is the intent of this work to identify the surface intermediates and reaction mechanisms for alcohols reacting on iron surfaces.

EXPERIMENTAL

The experiments were carried out in a stainless-steel ultrahigh vacuum chamber which has been described elsewhere (7). Briefly, the system contained 4-grid LEED optics, an X-ray source with a Mg anode, a quadrupole mass spectrometer, an argon ion source, a double pass cylindrical mirror analyzer with an integral electron gun, and a coolable crystal holder/manipulator. A clean Fe(100) sample, as verified by LEED, XPS, and Auger electron spectroscopy

(AES), was prepared by argon sputtering and high-temperature annealing as described elsewhere (7).

Samples of methanol, ethanol, and isopropanol were prepared by methods described elsewhere (8, 9). A gas manifold was filled to 20 Pa (0.150 Torr) with the desired gas and then admitted to the vacuum chamber through a 22-gauge needle, providing a highly collimated beam to the front face of the crystal. This means of exposing the crystal to a reactive gas allowed the front of the crystal to be completely covered maintaining the pressure in the chamber below 1.3×10^{-7} Pa, so that adsorption on the back side of the crystal could be neglected.

Sticking probabilities for the reactive gases were estimated relative to CO dosed under similar conditions. Adsorption was carried out with the crystal facing the collimating needle for 5 s with the valve opened to the manifold with a pressure of 20 Pa. The resulting coverage was estimated from XPS. CO dosed under these conditions was found to saturate the surface with 0.5 monolayers CO. The sticking probability of CO on Fe(100) at 180 K was found to be approximately one (7). Comparison of the coverage of the reactive gas to that obtained for CO provided an estimate of the sticking probability.

The reactions were followed by temperature-programmed reaction spectroscopy (TPRS) and X-ray photoelectron spectroscopy (XPS). With TPRS the evolution of products from the surface for the various reaction pathways was studied. Products were detected by the quadrupole mass spectrometer and verified against mass fragmentation patterns measured in our laboratory. Typically the reactant gas was adsorbed at or below 200 K, and the crystal was subsequently heated up to 1000 K by radiation from a tungsten filament located 3 mm behind the sample. Below 650 K the crystal was heated linearly with time at a rate of approximately 20 K/s; at higher temperatures the heating rate decreased

due to radiation losses. Data were taken with the aid of a DEC PDP 11-03 minicomputer interfaced to the mass spectrometer, which permitted five masses to be scanned simultaneously.

XPS was used to follow changes in the structure of the adsorbed intermediates. The procedure used to take the spectra is described in more detail elsewhere (7). Photoelectrons excited by X-rays supplied from a Mg anode (1254 eV) were collected by the CMA. Pulse counting of the collected electrons was done with the aid of a multichannel analyzer. Multiple scanning over a fixed energy range was employed to enhance the signal-to-noise ratio. A series of spectra of the C(1s) and O(1s) electron emission were taken after adsorption of the reactant at 200 K, heating to a specified temperature, and cooling again to 200 K to quench the reaction. Coverages of oxygen and carbon were determined by comparison of the O(1s) Fe(2p_{3/2}) and C(1s) Fe(2p_{3/2}) ratios to previously established calibration standards (12). The coverage determinations are accurate to ± 0.02 monolayers (2.4×10^{13} atoms/cm²). The binding energies were all referenced to the Fe(2p_{3/2}) transition, which has been determined to occur at 707.0 eV (11). The crystal was not moved when taking a series of spectra to assure that the observed changes were not due to variations across the crystal surface. The XPS spectra shown in the text are smoothed versions of digital data. Some drawing inaccuracies have resulted in the transcription process so that some peaks may appear slightly shifted from the peak energies quoted in the text. The XPS data given in the tables are more accurate, since they were obtained directly from the digital data. The figures are intended to convey the more qualitative features of the spectra.

RESULTS

The reactions of methanol, ethanol, and isopropanol were studied on Fe(100). The desorption products were monitored be-

tween 200 and 900 K with TPRS, while changes on the surface were checked by XPS. The sticking probabilities of methanol and ethanol on Fe(100) at 200 K were estimated to be near unity, with reference to CO. Isopropanol had a lower sticking probability of approximately 0.1. The primary reaction products of methanol and ethanol were CO and H₂, although alcohols, aldehydes, and hydrocarbons were also observed as reaction products. Isopropanol showed a low reactivity and primarily desorbed intact. XPS revealed that methanol caused slight oxidation of the Fe(100) surface, while ethanol and isopropanol caused carburization.

The reaction product spectra subsequent to CH₃OH adsorption at 200 K are shown in Fig. 1; other mass fragments were checked (e.g., 14, 15, 18, 29, 31, 44, 45, 60), but no other products were observed to desorb. CH₃OH and H₂CO were distinguished by the singly ionized parent molecule, *m/e* 32 and *m/e* 30 respectively, as CH₃OH does not have a significant *m/e* 30 fragment. CH₄ was determined from the *m/e* 16 fragment corrected for the O⁺ fragment of CO, which was unambiguously determined from the CO desorption at 800 K.

The data shown in Fig. 1 indicate the CH₄, CH₃OH, and H₂CO signals to be two orders of magnitude less than the CO and H₂ signals, however, these products were quite accurately identified. The sensitivity of the TPRS technique allows for product verification corresponding to less than 10⁻³ monolayers (1×10^{12} molecules), so that careful deconvolution of the mass spectral data can identify reaction products with widely varying yields. The product desorption spectra indicated four distinct reaction steps: (i) methanol desorption at 270 K; (ii) H₂ desorption at 350 K; (iii) the simultaneous desorption of CO, H₂, CH₃OH, H₂CO, and CH₄ at 450 K; (iv) CO desorption at 800 K. The desorption of CO at 800 K can be attributed to recombination and desorption of dissociated CO on the Fe(100) surface (7). To help unravel the

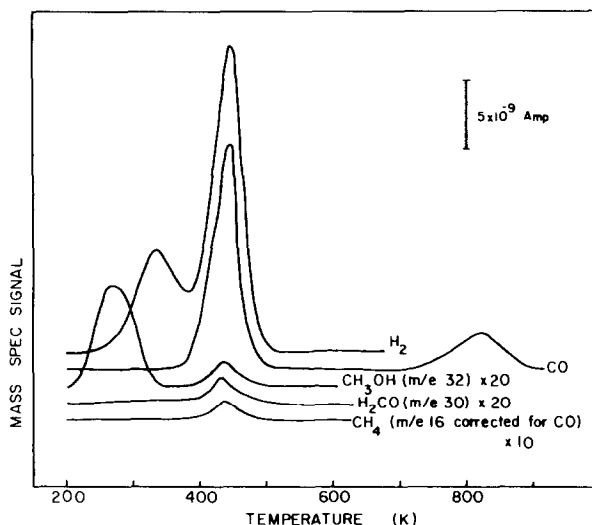


FIG. 1. Reaction products of methanol on Fe(100).

other reaction steps, a mixture of CH_3OD and CH_3OH was adsorbed on the Fe(100) surface (only the hydroxyl hydrogen was labeled, there was no exchange between the methyl and hydroxyl hydrogens). It was observed that CH_3OD (m/e 33) desorbed only at 270 K, while CH_3OH (m/e 32) desorbed at both 270 and 450 K. Additionally D_2 and HD and H_2 were observed as desorption products at 350 K, whereas only H_2 was observed to desorb at 450 K. These results indicated that methanol adsorbed on Fe(100) first lost its hydroxyl hydrogen, which desorbed at 350 K leaving adsorbed methoxy intermediates. The methoxy subsequently reacted to give CO, H_2 , H_2CO , CH_3OH , and CH_4 ; additionally some of the CO reaction product decomposed to adsorbed carbon and oxygen which recombined and desorbed at 800 K.

XPS helped to clarify some of the TPRS results. Figures 2 and 3 show the C(1s) and O(1s) X-ray photoelectron spectra for CH_3OH adsorbed on Fe(100) at 180 K, and subsequently heated to 350, 500, and 900 K. Before adsorbing methanol there was a slight carbon impurity (curve e) representing approximately 3% of a monolayer of carbon (1 monolayer = 1.2×10^{15} adsorbates/cm²). After adsorption of

CH_3OH at 180 K there was a single peak in the C(1s) spectrum at 285.6 eV and evidence for two peaks in the O(1s) spectrum one at 531.2 eV and a shoulder at approximately 532.0 eV. Saturation coverage of methanol adsorbed at 180 K was estimated from the XPS spectra to be 35% of a monolayer (see Table 1). After heating to 350 K there was a slight decrease in both the carbon and oxygen signals corre-

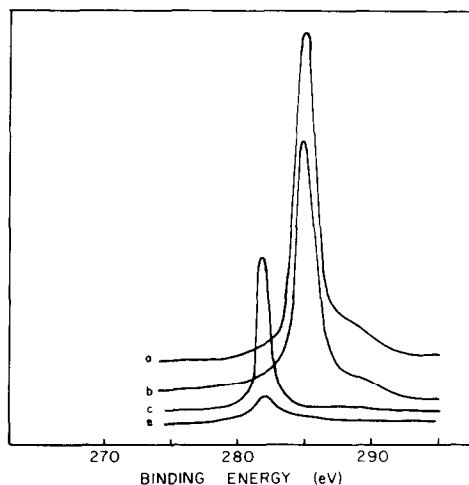


FIG. 2. C(1s) XPS for methanol adsorbed on Fe(100). (a) CH_3OH adsorbed at 180 K; (b) heated to 350 K; (c) heated to 500 K; (d) heated to 900 K—no peak visible; (e) before CH_3OH adsorption.

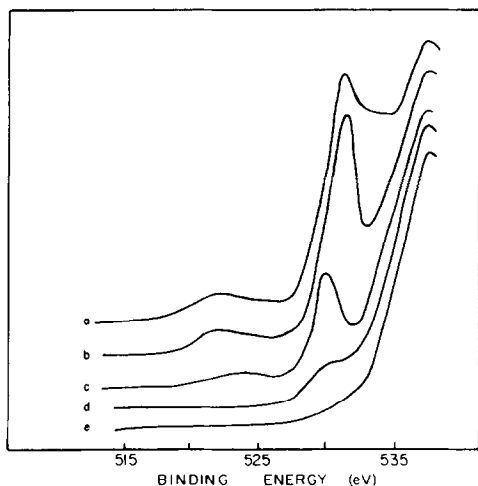


FIG. 3. O(1s) XPS for methanol adsorbed on Fe(100). (a) CH₃OH adsorbed at 180 K; (b) heated to 350 K; (c) heated to 500 K; (d) heated to 900 K; (e) before CH₃OH adsorption.

sponding to the desorption of approximately 5% of a monolayer of methanol at 270 K. The C(1s) peak showed a very slight shift in energy, while the O(1s) peak at 532.0 eV disappeared. These data suggested that there was a single species adsorbed on the surface above 350 K and that the O(1s) peak at 532.0 eV was due to undissociated methanol adsorbed on the surface.

Heating to 350 K caused the undissociated methanol to either desorb or react and form methoxy. It is important to note that the C(1s) spectra showed no evidence for CO dissociation after heating the surface to 350 K [there was no evidence for a C(1s) peak at 282.2 eV characteristic of surface carbon]. This finding indicated that decomposition of methanol to adsorbed carbon and oxygen did not occur at low temperature, and the dissociated CO, which desorbed at 800 K, was formed when the methoxy reacted at 450 K. The thermal dependence of the spectra and the C(1s) position was quite unlike that for CO adsorption (7, 11). The formation of the dissociated CO is seen in the XPS spectra taken after heating to 500 K. The C(1s) and O(1s) peaks emerged at 282.3 and 530.1 eV,

respectively. These binding energies corresponded to surface carbide and oxide characteristic of dissociated CO (7, 11). Finally, after heating to 900 K and XPS spectra showed the dissociated CO had desorbed. The results also showed that there was a small amount of oxygen buildup on the surface and depletion of the carbon contamination. The oxygen buildup observed was consistent with the formation of methane from the methoxy which required the formation of residual surface oxide. The amount of methane produced from the methoxy was estimated from the oxygen buildup to be approximately 17% of the reaction product from the methoxy (from Table 1 the net oxygen buildup was 0.05 monolayers and the amount of methoxy was 0.30 monolayers). The XPS results for methanol adsorbed on Fe(100) are summarized in Table 1 which gives the major peak positions and the total atomic coverage of carbon and oxygen corresponding to each spectrum.

Information concerning the reaction kinetics was obtained from the variation of peak positions with coverage and heating rate. The CO and H₂ product desorption spectra as a function of methanol coverage are shown in Fig. 4. The CO and H₂ product desorption peaks at 450 K showed no dependence on coverage, indicative of a first-order process. The activation energy and frequency factor for this reaction step were determined from the variation of peak tem-

TABLE I
Methanol Adsorption on Fe(100)

	Binding energies (eV)		Coverages (monolayers)	
	O(1s)	C(1s)	θ_c	θ_o
(a) CH ₃ OH adsorbed at 200 K	532.0 531.2		0.40	0.35
(b) Heated to 350 K	531.2	285.4	0.33	0.29
(c) Heated to 500 K	530.1	282.2	0.12	0.13
(d) Heated to 900 K	530.1	—	—	0.02
(e) Clean surface	—	282.2	0.03	—
(f) Molecular CO on Fe(100)	—	284.8	—	—

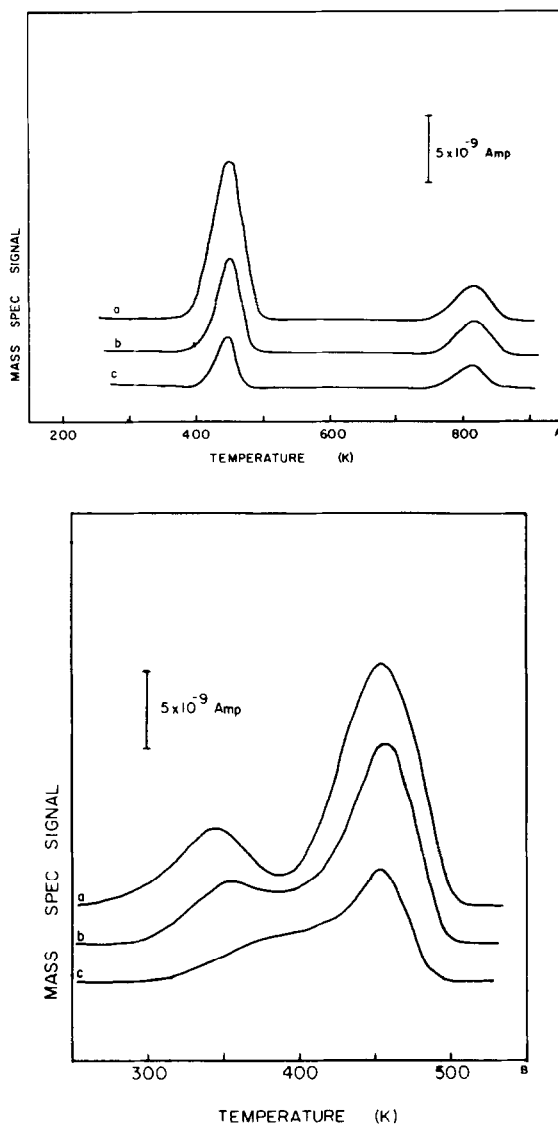


FIG. 4. (A) CO/CH₃OH coverage variation. (B) H₂/CH₃OH coverage variation. (a) $\theta_{\text{CH}_3\text{OH}} = 0.35$ monolayers; (b) $\theta_{\text{CH}_3\text{OH}} = 0.20$ monolayers; (c) $\theta_{\text{CH}_3\text{OH}} = 0.12$ monolayers.

perature with heating rate (28). The heating rate was varied between 6 and 26 K/s with the peak temperature varying between 430 and 451 K; the data gave an activation energy of 105 kJ/mole and a frequency factor of $4 \times 10^{12} \text{ s}^{-1}$. Another interesting feature shown in Fig. 4B was the shift of the low temperature H₂ peak with increasing methanol coverage. This shift in peak temperature paralleled that for H₂/H₂ (7), indicating that the hydroxyl hydrogen was lost

at low temperature and desorbed by a desorption limited step.

Ethanol reacted on Fe(100) in an analogous fashion to methanol. The reaction product spectra from CH₃CH₂OD adsorbed at 200 K are shown in Fig. 5. CO and H₂ were the major desorption products, desorbing simultaneously at 420 K, along with CH₄, C₂H₄, CH₃CHO, and CH₃CH₂OH. The hydroxyl hydrogen, which was isotopically labeled, desorbed at 325 K; and the

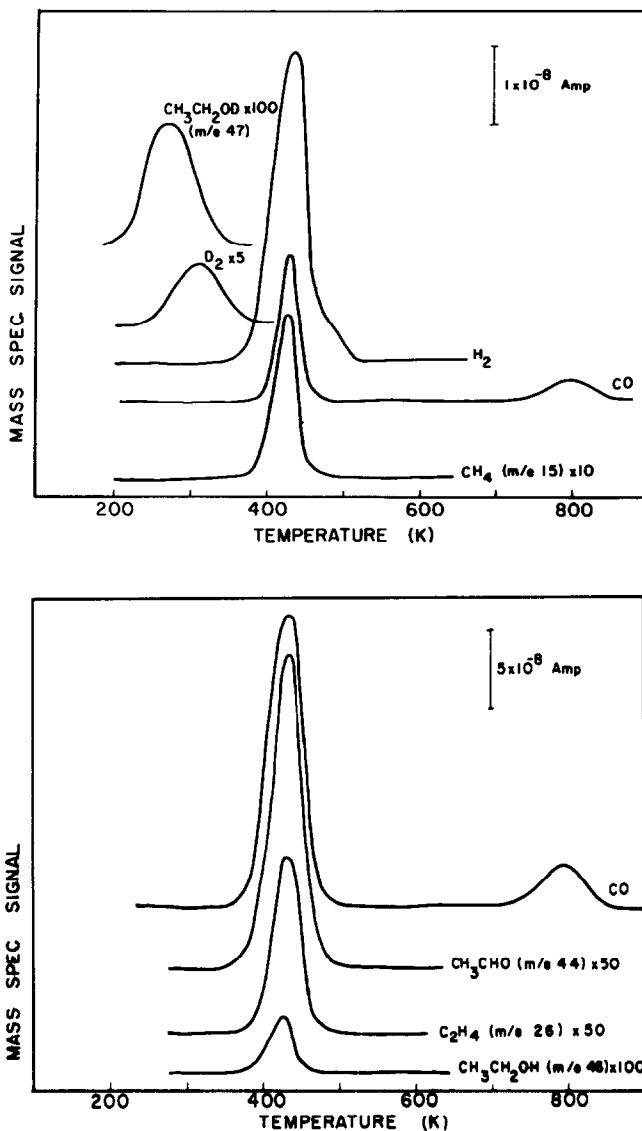


FIG. 5. Reactions of ethanol-OD on Fe(100).

parent molecule, $\text{CH}_3\text{CH}_2\text{OD}$, desorbed at 270 K. [All these products were clearly identified by their mass fragmentation patterns except ethylene (C_2H_4). Ethylene was identified from m/e 25 and 26 peaks at 420 K. There was also an m/e 30 fragment peak at 420 K which was about 20% of the m/e 26 fragment, which suggested that there may have been a mixture of ethane and ethylene. Because of the large number of products desorbing it was not possible to

definitively distinguish ethylene and ethane, but it was apparent that hydrocarbon products were formed.] The reaction scheme suggested by these data is adsorption of ethanol, loss of the hydroxyl hydrogen and formation of ethoxy intermediates, and the reaction of ethoxy to form CO and H_2 , as well as CH_4 , CH_3CHO , $\text{CH}_3\text{CH}_2\text{OH}$, and C_2H_4 (C_2H_6). An interesting feature to note is that much more methane was formed from the reactions of ethoxy than

the reactions of methoxy, there being almost an order of magnitude difference (compare CH_4/CO peak ratios in Figs. 1 and 5).

The kinetic parameters for the reactions of ethoxy on Fe(100) were determined by the same techniques used for methoxy decomposition. Coverage variation studies showed that the CO and H_2 desorption peaks at 420 K did not shift with ethoxy coverage indicating a first-order reaction process. An activation energy of 111 kJ/mole and frequency factor of $8 \times 10^{13} \text{ s}^{-1}$ were determined for the reaction of ethoxy from the variation in peak position with heating rate.

The XPS data for ethanol adsorbed on Fe(100) also paralleled the XPS data for methanol adsorption. The C(1s) spectra shown in Fig. 6 showed that ethanol adsorption at 200 K resulted in a broad peak at 285.1 eV (the shoulder at 282 eV was due to carbon contamination on the surface present before adsorption). The breadth of this peak indicated that it resulted from a combination of two peaks, most probably representing the two different carbons in ethanol. No change was seen in these peaks upon heating to 350 K except for a slight

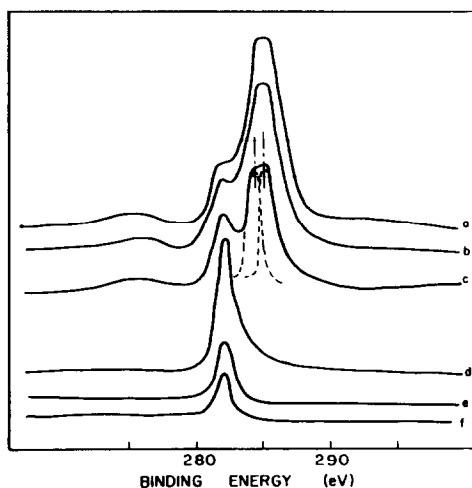


FIG. 6. C(1s) XPS for ethanol adsorbed on Fe(100). (a) $\text{CH}_3\text{CH}_2\text{OD}$ adsorbed at 200 K; (b) heated to 280 K; (c) heated to 350 K; (d) heated to 500 K; (e) heated to 900 K; (f) before adsorption.

TABLE 2
Ethanol Adsorption on Fe(100)

	Binding energies (eV)		Coverages (monolayers)	
	C(1s)	O(1s)	θ_c	θ_o
(a) $\text{CH}_3\text{CH}_2\text{OD}$ adsorbed at 200 K	281.9 285.1	531.4	0.52	0.23
(b) Heated to 280 K	282.0 285.1	531.2	0.42	0.20
(c) Heated to 350 K	282.1 284.5 285.5	531.1	0.40	0.19
(d) Heated to 500 K	282.2	530.1	0.13	0.06
(e) Heated to 900 K	282.2	—	0.08	—
(f) Before adsorption	282.2	—	0.06	—
(g) Molecular CO on Fe(100)	284.8	—	—	—

decrease in intensity due to ethanol desorption at 270 K. The separation of these peaks was approximately 1 eV as indicated in spectrum c where the two different peaks are sketched in. The C(1s) peak at higher energy was at approximately the same energy as the C(1s) peak for methoxy (285.4 eV), which suggested that it was due to the carbon bonded to the oxygen, while the peak at lower energy could be assigned to the methyl carbon. After heating to 500 K the peaks at 285 eV disappeared, and the only carbon peak left was at 282.2 eV, characteristic of surface carbon and dissociated CO. Heating to 900 K caused desorption of dissociated CO resulting in a decrease in the C(1s) intensity. The overall adsorption/reaction cycle resulted in carbon buildup on the surface (compare spectra e and f and see Table 2).

The O(1s) spectra, shown in Fig. 7, showed one striking difference from the C(1s) spectra. For ethanol adsorbed at 200 K there was evidence for two peaks in the O(1s) spectrum, one at 531.2 eV and a shoulder at approximately 532.0 eV. Heating to 350 K caused the higher binding energy peak to diminish. The same behavior was also noted for methanol adsorption on Fe(100).

The results for isopropanol adsorption on Fe(100) were rather surprising after seeing such similarity between methanol and etha-

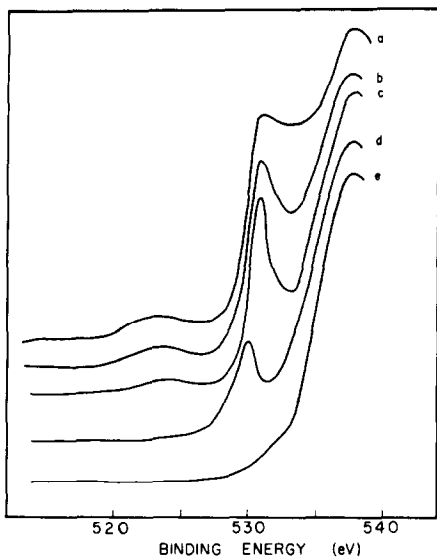


FIG. 7. O(1s) XPS for ethanol adsorbed on Fe(100). (a) $\text{CH}_3\text{CH}_2\text{OD}$ adsorption at 200 K; (b) heated to 280 K; (c) heated to 350 K; (d) heated to 500 K; (e) heated to 900 K; (f) before adsorption—same as (e).

nol. The reaction product spectra following isopropanol adsorption at 160 K are shown in Fig. 8. In striking contrast to methanol and ethanol adsorption on Fe(100) where 70–80% of the adsorbed alcohol reacted to form an alkoxy which in turn reacted above

400 K, only 10% of the adsorbed isopropanol reacted to form species which remained on the surface above 300 K. Most of the isopropanol was observed to desorb at 225 K, along with CO , H_2 , and CH_4 . The only other desorption products were H_2 which desorbed at 400 and 470 K, $(\text{CH}_3)_2\text{CO}$ which desorbed at 400 K, and $\text{CO}(\beta)$ which desorbed at 800 K. The products desorbing above 300 K were identical to what was observed for acetone adsorbed on Fe(100), suggesting that acetone and isopropanol formed a common intermediate. The reaction products for this intermediate were different from the alkoxy intermediates derived from methanol and ethanol in that neither hydrocarbons, alcohols, nor CO were observed to desorb above 300 K. The identity of this intermediate is unknown.

The XPS results shown in Figs. 9 and 10 clearly showed that almost all the adsorbed isopropanol desorbed below 300 K. The C(1s) spectrum for isopropanol adsorbed at 160 K showed a large peak at 284.4 eV with a smaller peak at 285.7 eV. These correspond to the two different carbon species found in isopropanol and occur in a ratio of

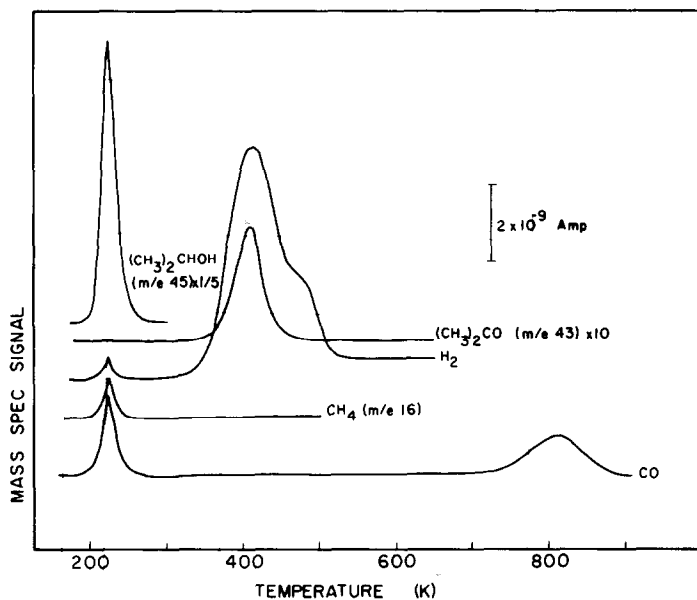


FIG. 8. Reactions of isopropanol on Fe(100).

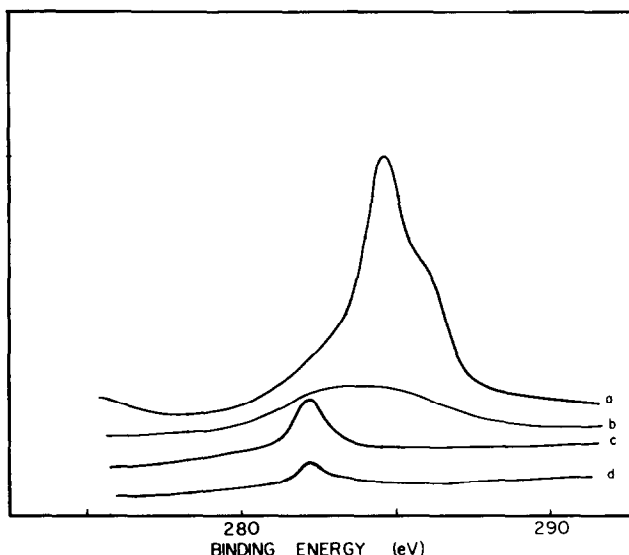


FIG. 9. C(1s) XPS for isopropanol adsorbed on Fe(100). (a) $(\text{CH}_3)_2\text{CHOH}$ adsorbed at 160 K; (b) heated to 300 K; (c) heated to 500 K; (d) heated to 900 K.

2:1. These peaks can be assigned to the two different carbons as was done for ethanol. The 284.4 peak corresponded to the methyl groups bonded to another carbon, which was nearly the same energy observed for the equivalent carbon in ethanol.

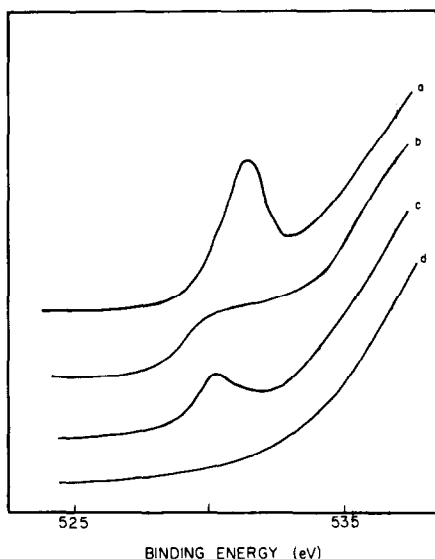


FIG. 10. O(1s) XPS for isopropanol adsorbed on Fe(100). (a) $(\text{CH}_3)_2\text{CHOH}$ adsorbed at 160 K; (b) heated to 300 K; (c) heated to 500 K; (d) heated to 900 K.

The peak at 285.7 eV corresponded to the carbon bonded to the oxygen, in agreement with the assignment for methanol and ethanol. The O(1s) spectrum for isopropanol adsorbed at 160 K showed a single peak at 531.4 eV. When the surface was heated to 300 K, both the C(1s) and O(1s) intensities were greatly diminished due to isopropanol desorption. Because so little material remained adsorbed on the surface, the XPS signals were too small to identify accurately any other species other than some atomic oxygen and carbon. The final spectra taken after heating to 900 K revealed carbon buildup on the surface due to isopropanol decomposition. The XPS data for isopropanol adsorption on Fe(100) are summarized in Table 3.

DISCUSSION

The reactions of methanol and ethanol on Fe(100) showed that stable alkoxy intermediates were formed. These results agreed with the ir work of Blyholder and Neff (6) in which stable alkoxy intermediates were also observed. Furthermore Blyholder and Neff identified that the alkoxy intermediates were not stable at 450 K as observed here. We have also

TABLE 3
Isopropanol Adsorption on Fe(100)

	Binding energies (eV)		Coverages (monolayers)	
	O(1s)	C(1s)	θ_c	θ_o
(a) $(\text{CH}_3)_2\text{CHOH}$ adsorbed at 160 K	531.4	284.4 285.7	0.46	0.16
(b) Heated to 300 K	—	—	0.09	0.04
(c) Heated to 500 K	530.1	282.2	0.07	0.03
(d) Heated to 900 K	—	282.2	0.03	—
(e) Molecular CO on Fe(100)	—	284.8	—	—

identified the reaction products from the reactions of alkoxys on iron and the kinetics of these reactions.

The identification of surface alkoxys has now been established on a wide variety of surfaces. (These intermediates are also referred to as alkoxides, particularly when dealing with acid-base type reactions.) Methoxide was found to be the stable surface intermediate on a ZnCrCu catalyst for methanol synthesis from a CO/H_2 reactant gas mixture (13-15). Ethoxide was observed to result from ethanol and diethyl ether adsorption on alumina catalysts (16-20), and methoxide was observed on alumina (21), magnesia (22), and an iron-molybdenum oxide catalyst (23). The reactions of the alkoxys on these catalysts were similar to those on Fe(100) in that CO and H_2 were major decomposition products, with lesser amounts of hydrocarbons and aldehydes. A major difference was that on the oxide catalysts ethers were observed as reaction products, whereas on Fe(100) no such products were observed.

Alkoxys have also been identified on a variety of transition metal surfaces as well. Wachs and Madix observed that alkoxys were the stable surface intermediates in the oxidation of alcohols to aldehydes on Cu(110) and Ag(110) (8, 24). An alkoxy intermediate was also observed from the reactions of methanol on W(100) (25). In addition Blyholder and Wyatt (26) have identified alkoxys on Cobalt using infrared spectroscopy. The only metal studied on

which a stable alkoxy did not seem to form was nickel. Johnson (27) and Blyholder and Neff (28) have both observed that alcohols decomposed below room temperature to CO and hydrogen on nickel. Demuth and Ibach (29) also obtained this result for methanol on Ni(111); however, they also identified a methoxy intermediate at low temperature.

The reason for the difference in stabilities of surface alkoxides is not well understood. Blyholder and Wyatt (26) have suggested that the difference in the stability of alkoxys on iron and nickel was due to the difficulty in forming strong $\text{M}-\text{OR}$ bonds with metals of nearly filled nickel d-bands. The stability of alkoxys on Cu and Ag is contrary to this hypothesis, however. It is more likely that the relative stabilities of the alkoxides is strongly related to both the oxygen-metal and hydrogen-metal bond strengths, since the alkoxide decomposes by hydrogen atom transfer to the surface. Whatever the cause of this difference between iron and nickel, an important consequence is reflected in their catalytic behavior. Hydrogenation of CO over nickel produces primarily methane, with almost no oxygenated products, whereas iron catalysts produced significant amounts of alcohols and long chained hydrocarbons (3, 5).

The results of this study coupled with previous studies suggest that alkoxys are important intermediates in the Fischer-Tropsch synthesis. The importance of alcohol related intermediates to Fischer-Tropsch synthesis was demonstrated by Kummer and Emmett (4). They added radioactive labeled alcohols to a CO/H_2 feed stream over iron catalysts to see how they were incorporated into the products of Fischer-Tropsch synthesis. Primary alcohols were found to be almost completely incorporated into longer chained hydrocarbons, while secondary alcohols were incorporated to a much lower extent, and tertiary alcohols were totally inactive. The work reported here clearly shows that alcohols adsorbed on iron to form alkoxy intermedi-

ates, and furthermore, that the alkoxys reacted to give hydrocarbon products [e.g., CH_4 and C_2H_4 (C_2H_6) were both observed as reaction products from ethoxy on $\text{Fe}(100)$]. This observation provides the necessary link between alkoxys and the Fischer-Tropsch reaction products. Other intermediates may be important as well, of course.

A final point that should be mentioned is the apparent difference in the reactions of primary and secondary alcohols. In this study it was observed that methanol and ethanol, which are primary alcohols, formed stable alkoxy intermediates. Both of these alkoxys reacted at temperatures above 400 K. Isopropanol however behaved differently and did not seem to form a stable alkoxy intermediate readily. These results agree with the results of Kummer and Emmett cited above which showed that secondary alcohols were not incorporated into Fischer-Tropsch products to the extent that primary alcohols were. Blyholder and Neff (6) also concluded that secondary alcohols were not adsorbed as strongly as primary alcohols. One possible explanation for the low stability of secondary alkoxys is the steric interference of the methyl groups with the surface, as indicated in Fig. 11. Normal alcohols would assume configuration (a) to minimize the interactions between the substituents bonded to the carbon and the surface. However, if bound, secondary alcohols, with two bulky substituent groups, would assume configuration (b) so the R groups were as far from the surface as possible [note that if CH_3 were substituted for one of the H's in

(a) the hydrogens of the methyl group would penetrate the plane of the surface]; this arrangement would also cause the hydrogen bound to the secondary carbon to be pushed toward the surface reducing the stability of the alkoxy. These observations are also consistent with Kummer and Emmett's work showing secondary alcohols are not incorporated into hydrocarbon products as readily as primary alcohols. Furthermore the extension of these arguments to tertiary alcohols indicates they should not form surface alkoxys, which is consistent with Kummer and Emmett's observation that tertiary alcohols were inactive when added to a CO/H_2 feed stream.

ACKNOWLEDGMENTS

The authors gratefully acknowledge the support of the National Science Foundation through grant NSF Eng 77-12964 and for equipment through grant NSF Eng 75-14191. Without this support the work could not have been accomplished.

REFERENCES

1. Streitweiser, A., Jr., and Heathcock, C. H., in "Introduction to Organic Chemistry." McMillan, New York, 1976.
2. Madix, R. J., and Benziger, J., *Annu. Rev. Phys. Chem.* **XXIX**, 284 (1978).
3. Anderson, R. B., in "Catalysis" (P. H. Emmett, Ed.), Vol. IV. Reinhold, New York, 1956; and references therein.
4. Kummer, J. T., and Emmett, P. H., *J. Amer. Chem. Soc.* **75**, 5177 (1953).
5. Storch, H. H., Golumbic, N., and Anderson, R. B., in "The Fischer Tropsch and Related Syntheses." Wiley, New York, 1951.
6. Blyholder, G., and Neff, L. D., *J. Phys. Chem.* **70**, 893 (1966).
7. Benziger, J. B., Ph.D. Thesis, Stanford University, 1979.
8. Wachs, I. E., and Madix, R. J., *J. Catal.* **53**, 208 (1978).
9. Johnson, S. W., and Madix, R. J., to be published.
10. "Atlas of Mass Spectral Data," (E. Stenhagen, S. Abrahamson, and F. W. McLafferty, Eds.), Vol. 1. Interscience, New York, 1969.
11. Brundle, C. R., *IBM J. R D* **22**, 235 (1978).
12. Benziger, J. B., and Madix, R. J., *J. Elec. Spectrosc. Related Phenomena*, submitted.
13. Tsuchiya, S., and Shiba, T., *J. Catal.* **4**, 116 (1956).

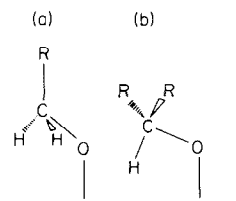


FIG. 11. Schematic drawing of primary and secondary alkoxides adsorbed on a surface.

14. Tsuchiya, S., and Shiba, T., *J. Catal.* **6**, 270 (1966).
15. Borowitz, J. L., *J. Catal.* **13**, 106 (1969).
16. Arai, H., Take, J.-I., Saito, V., and Yoneda, Y., *J. Catal.* **9**, 146 (1967).
17. Arai, H., Saito, and Yoneda, Y., *Bull. Chem. Soc. Japan* **40**, 731 (1967).
18. Schwarb, G. M., Jeukner, O., and Leitenberger, W., *Z. Electrochem.* **63**, 461 (1959).
19. Jain, J. R., and Pillai, C. N., *J. Catal.* **9**, 322 (1967).
20. Arai, H., Saito, Y., Yoneda, Y., *J. Catal.* **44**, 128 (1976).
21. Matsushima, T., and White, J. M., *J. Catal.* **44**, 183 (1976).
22. Foyt, D. C., and White, J. M., *J. Catal.* **47**, 260 (1977).
23. Edwards, J., Nicolaidis, J., Cutlip, M. B., and Bennett, C. O., *J. Catal.* **50**, 24 (1977).
24. Wachs, I. E., and Madix, R. J., *Surface Sci.* **76**, 531 (1978).
25. Ko, E. I., Benziger, J. B., and Madix, R. J., *J. Catal.* **62**, 264 (1980).
26. Blyholder, G., and Wyatt, W. V., *J. Phys. Chem.* **70**, 1745 (1966).
27. Johnson, S. W., Ph.D. thesis, Stanford University, 1979.
28. Blyholder, G., and Neff, L. D., *J. Phys. Chem.* **70**, 1738 (1966).
29. Demuth, J. E., and Ibach, H., *Chem. Phys. Lett.* **60**, 395 (1979).